The nucleon momentum and density distribution of the 4He nucleus using the Morse potential

K. Ypsilantis, S. Dimitrova, C. Koutroulos, M. Grypeos, A. Antonov

doi: 10.12681/hnps.2918

The nucleon momentum and density distribution of the ^4He nucleus using the Morse potential

K. Ypsilantis [a], S. Dimitrova [a,c], C. Koutroulos [a], M. Grypeos [a] and A. Antonov [b]

[a] *Department of Theoretical Physics Aristotle University of Thessaloniki, Greece*

[b] *Bulgarian Academy of Sciences Institute of Nuclear Research and Nuclear Energy, Sofia, Bulgaria.*

[c] *Bulgarian Academy of Sciences Institute of Nuclear Research and Nuclear Energy, Sofia, Bulgaria.*

Abstract

The nucleon momentum and density distribution of the ^4He nucleus are calculated by using the Morse single-particle potential. The parameters for the momentum distribution $n(k)$ are determined by fitting either the charge form factor to the available experimental data of the elastic electron scattering by ^4He or the momentum distribution to the corresponding "experimental" values. The calculations can be performed partly analytically and the results show a considerable overall improvement with respect to those obtained with the oscillator shell model. The r.m.s radius of the charge density distribution determined by fitting the charge form factor is in very good agreement with the values obtained by means of model independent analysis.

1 Introduction

The nucleon momentum distribution $\eta(k)$ in ^4He [1-3] has received considerable attention by quite a number of authors who used various theoretical approaches. One of the main reasons is the simplicity of this nucleus. Moreover, ^4He is one of the very few nuclei for which "experimental" values of $\eta(k)$ are available [4] so that there is a means of checking out each method.

Among the methods which have been used in calculations of the momentum distribution of nuclei, those based on many-body techniques are usually the most satisfactory ones. They are, however, more complex than those based on

single particle models. As is well known, the disadvantage of the latter is that, one cannot fit with such a model both the form factor and the momentum distribution. Thus, if the parameters are determined by fitting the theoretical charge form factor to the corresponding experimental results, the values of the momentum distribution are not expected to agree well with the experimental values of $\eta(k)$. Nevertheless, the choice of the single particle potential seems to play an important role in improving the results and diminishing the above mentioned discrepancy between the calculated and experimental values of $\eta(k)$. This is clear if a strong short range repulsion is included in the potential. If for example a potential of the form [5]

$$V(r) = -V_0 + \frac{1}{2}kr^2 + \frac{B}{r^2}, \quad 0 \leq r < \infty \tag{1}$$

$k > 0, \quad B > 0$ is used, then a considerable improvement is mostly observed not only for the form factor but also for the momentum distribution.

A characteristic of potential (1) is that it has an "infinite soft core" near the origin, which seems to be an extreme. It is more natural to expect that there is a repulsion in the single particle potential near the origin, as for example relativistic Hartree calculations indicate, but not with an infinite behaviour near the origin. Thus, a potential of the Morse type [6-12] which, as is well known, has many applications in Physics, might be appropriate as a first approximation to the single-particle potential of a light nucleus. The disadvantage is that the Schrödinger eigenvalue problem can be solved analytically only for the s-states for this potential. Therefore, it is not so convenient to use for heavier nuclei if one wishes to take advantage of its analytic properties.

In the next section the notation is specified and basic formulae regarding the Schrödinger eigenvalue problem with the Morse potential are given. In section 3, the expressions of the density distribution and its m.s. radius, the form factor and momentum distribution are given. The final section is devoted to the numerical results, comments and conclusions.

2 The exact and approximate single-particle s-state wave functions

The well-known Morse potential is given by the following expression [6]:

$$V(r) = D[e^{-2a(r-r_0)} - 2e^{-a(r-r_0)}] = -D + D[1 - e^{-a(r-r_0)}]^2,$$

$$0 \leq r < \infty. \tag{2}$$

It has its minimum value $(-D)$ at $r = r_0$, tends assymptotically to zero as $r \to \infty$ and is repulsive near the origin taking the value $De^{2ar_0}(1 - 2e^{-ar_0})$ at $r = 0$. The corresponding radial Schröndinger equation for the s-state wave functions $\phi_{n0}(r) = rR_{n0}(r)$, may be written in the form [7,8]

$$y^2\frac{d^2\phi_{n0}}{dy^2} + y\frac{d\phi_{n0}}{dy} + (-\frac{\beta^2}{a^2} + \frac{\gamma}{a}y - \frac{1}{4}y^2)\phi_{n0} = 0, \tag{3}$$

where

$$\beta^2 = -\frac{2\mu}{\hbar^2}E, \quad \gamma^2 = \frac{2\mu}{\hbar^2}D = d^2a^2 \quad and \quad y = \frac{2\gamma}{a}e^{-a(r-r_0)}, \tag{4}$$

The differential equation (3) has singularities at $y = 0$ and $y = \infty$. By setting (in view of the asymptotic behaviour at the boundaries):

$$\phi_{n0}(y) = y^{\beta/a}e^{-y/2}F(y), \tag{5}$$

one obtains a differential equation for $F(y)$

$$yF'' + (c - y)F' - \lambda F = 0, \tag{6}$$

where

$$c = \frac{2\beta}{a} + 1, \quad \lambda = \frac{1}{2}c - \frac{\gamma}{a}. \tag{7}$$

Eq. (6) is of the standard form of the confluent hypergeometric differential equation with the exact solution

$$F(y) = A_{n0} \cdot {}_1F_1(\lambda; c; y) + B_{n0} \cdot y^{1-c}{}_1F_1(\lambda - c + 1; 2 - c; y). \tag{8}$$

To satisfy the boundary condition $\phi_{n0} = 0$ for $r \to \infty$ or $y = 0$, the constant B_{n0} is bound to vanish since the exponent of y is negative. So, the exact wave function becomes:

$$\phi_{n0}(y) = A_{n0}y^{\beta/a}e^{-y/2}{}_1F_1(\lambda; c; y). \tag{9}$$

The constant A_{n0} is to be fixed by the normalization condition.

The second boundary condition, $\phi_{n0} = 0$ at $r = 0$, or $y = y_0 = \frac{2\gamma}{a}e^{ar_0}$ leads to the following transcendental equation for the energy eigenvalues:

$$ {}_1F_1(\lambda; c; y_0) = 0. \tag{10}$$

Equation (10) has to be solved numerically in order to determine the bound s-state energies and subsequently the corresponding eigenfunctions.

An approximate analytic expression for the energy eigenvalues E_{n0} may be obtained [7,8] from (10) if y_0 turns out to be sufficiently large so that one can use the asymptotic expression of ${}_1F_1$. Such a condition is reasonably well satisfied for the numerical values of the parameters of the Morse potential, typical for the ^4He nucleus, when these are determined by fitting the charge form factor (see last section). It should be also noted that the case of very large $y_0 (y_0 \to \infty)$ leads to the same eigenvalues which result if the boundary condition was not $\phi_{nl}(0) = 0$ but $\phi_{nl}(-\infty) = 0$. Therefore the condition that y_0 be very large leads to eigenvalues E_{n0} which are the same as those appearing in the corresponding one-dimensional eigenvalue problem. In view of the previous remarks we may write

$$ {}_1F_1(\lambda, c; y_0) \simeq \frac{\Gamma(c)}{\Gamma(\lambda)} e^{y_0} y_0^{\lambda - c} = 0 \tag{11}$$

Therefore $\Gamma(\lambda) = \infty$ and $\lambda = -n, \quad n = 0, 1, 2, \ldots$ Consequently, the approximate energy eigenvalues are given by the expression: (derived originally by Morse [6]):

$$ E_{n0} = -\frac{\hbar^2}{2\mu}\beta^2 = -\frac{\hbar^2}{8\mu}a^2(2d-1-2n)^2 = -D + \hbar\omega_0(n+\frac{1}{2}) - \frac{\hbar^2\omega_0^2}{4D}(n+\frac{1}{2})^2 \tag{12}$$

where the integer n is in the interval $0 \leq n \leq (\frac{2d-1}{2})$ and ω_0 is the angular frequency of the classical small vibrations around r_0:

$$ \omega_0 = a(\frac{2D}{\mu})^{1/2} \tag{13}.$$

In the present case the analytic expression of the corresponding eigenfunctions is simplified since the confluent hypergeometric function in (9) becomes a polynomial. Thus we obtain

$$ \phi_{n0}(r) = N_{n0} e^{-de^{-a(r-r_0)}} e^{-\frac{a}{2}(2d-1-2n)(r-r_0)} \cdot L_n^{2d-1-2n}(2de^{-a(r-r_0)}) \tag{14},$$

where the normalization factor N_{n0} is given by

$$ N_{n0} = [A_{n0}(2d)^{\frac{1}{2}(2d-1-2n)} n! \Gamma(2d-2n)/\Gamma(2d-n)]$$

and the generalized Laguerre Polynomials $L_n^\delta(y)$ are defined by $L_n^\delta(y) = e^y \frac{y^{-\delta}}{n!} \frac{d^n}{dx^n} e^{-y} y^{n+\delta}$.It should be noted that this definition of L_n^δ, which is the more commonly used, differs somewhat from that used by Morse [6].

The approximate ground-state radial wave function in which we are interested here is given by the expression:

$$\phi_{00}(r) = N_{00} e^{-de^{-a(r-r_0)}} e^{-\frac{a}{2}(2d-1)(r-r_0)}, \tag{15}$$

where the normalization constant N_{00} is expressed in terms of the parameters a and d as follows:

$$N_{00} = [\frac{a(2d)^{2d-1}}{\Gamma(2d-1)}]^{\frac{1}{2}}. \tag{16}$$

In the present calculations we are using both, the exact and the approximate solutions of eq. (3).

3 Expressions for the density distribution, the form factor and the nucleon momentum distribution in ^4He.

In this section we give the expressions of the density distribution, its m.s. radius, the form factor and the momentum distribution of ^4He.

The normalized to unity ($\int \rho(r) d^3r = 1$) density distribution in the single particle model is given by the general expression [1]

$$\rho(r) = \frac{1}{4\pi Z} \sum_{nlj}^{(nlj)_F} (2j+1) |R_{nlj}(r)|^2 \tag{17}.$$

Thus, in the case of the ^4He we have simply ($R_{001/2} \rightarrow R_{00}$)

$$\rho(r) = \frac{1}{4\pi} |R_{00}(r)|^2 \tag{18}$$

The point-proton form factor in the Born approximation and for spherically symmetric $\rho(r)$ is:

$$F(q) = 4\pi \int_0^\infty \rho(r) (\frac{sinqr}{qr}) r^2 dr \tag{19}$$

In the case of ^4He we have

$$F(q) = \int_0^\infty |R_{00}(r)|^2 (\frac{sinqr}{qr}) r^2 dr \tag{20}$$

The proton form factor is introduced using the Chandra and Sauer parametrization [13]

$$f_p(q) = \sum_{i=1}^{3} A_{p_i} e^{-\frac{a_{p_i}^2 q^2}{4}} \tag{21}$$

where

$$A_{p_1} = 0.506373, A_{p_2} = 0.327922, A_{p_3} = 0.165705$$

and

$$a_{p_1}^2 = 0.431566 fm^2, a_{p_2}^2 = 0.139140 fm^2, a_{p_3}^2 = 1.52554 fm^2$$

The center of mass correction in the Form Factor of ^4He is taken into account, using the "fixed center of mass correction" of Radhakant-Khadkikar-Banerjee [14]. Thus, the expression of the form factor corrected for the center of mass motion is:

$$\tilde{F}(q) = \frac{\int d^3\omega F(|\vec{q} + \vec{\omega}|) F^3(\omega)}{\int d^3\omega F^4(\omega)} \tag{22}$$

Therefore the theoretical expression for the charge form factor is:

$$F_{ch}(q) = f_p(q) \cdot \tilde{F}(q) \tag{23}$$

The normalized to unity nucleon momentum distribution $\int \eta(k) d^3k = 1$, for a nucleus, in the single particle model is given by the general expression [1] :

$$\eta(k) = \frac{1}{4\pi Z} \sum_{nlj}^{(nlj)_F} (2j+1) |\tilde{R}_{nlj}(k)|^2 \tag{24}$$

where

$$\tilde{R}_{nlj}(k) = (\frac{2}{\pi})^{1/2} (-i)^l \int_0^\infty dr r^2 j_l(kr) R_{nlj}(r); \tag{25}$$

Thus, in the case of the ^4He we have simply:

$$\eta(k) = \frac{1}{4\pi} |\tilde{R}_{00}(k)|^2 \tag{26}$$

where

$$\tilde{R}_{00}(k) = (\frac{2}{\pi})^{1/2} \int_0^\infty dr r^2 j_0(kr) R_{00}(r) \qquad (27).$$

The m.s. radius of the density distribution is calculated from the formula

$$< r^2 >= \frac{\int_0^\infty r^2 \rho(r) d^3 r}{\int_0^\infty \rho(r) d^3 r} \qquad (28)$$

The above formulae if the approximate wave-function of the Morse potential is used, read as follows for ^4He

$$\rho(r) = \frac{1}{4\pi} \frac{1}{r^2} [\frac{a(2d)^{2d-1}}{\Gamma(2d-1)}] e^{-2de^{-a(r-r_0)}} e^{-a(2d-1)(r-r_0)} \qquad (29)$$

$$F(q) = \frac{1}{q} [\frac{a(2d)^{2d-1}}{\Gamma(2d-1)}] \int_0^\infty \frac{1}{r} dr sin(qr) e^{-2de^{-a(r-r_0)}} e^{-a(2d-1)(r-r_0)} \qquad (30)$$

$$\eta(k) = \frac{1}{2(\pi k)^2} \frac{a(2d)^{2d-1}}{\Gamma(2d-1)} | \int_0^\infty dr sin(kr) e^{-de^{-a(r-r_0)}} e^{-a(d-\frac{1}{2})(r-r_0)} |^2 \qquad (31)$$

The integrations in (30) and (31) are performed numerically.

4 Numerical results, comments and conclusions

Calculations of the form factor, the nucleon momentum distribution, the point-proton (or body) and charge density distributions and their root mean square radii were performed for ^4He using the exact as well as the approximate solutions of the Schrödinger equation. In these calculations the center of mass correction was taken into account either by using the Radhakant-Khadkikar-Banerjee (RKB) correction, in which case in the formulae the ordinary nucleon mass m is used or by using simply the reduced mass μ. The potential parameters were determined by the least-squares method either by fitting the theoretical expression of the charge form factor to the experimental data or by fitting the theoretical expression of the momentum distribution to the corresponding "experimental" data. We note that some preliminary results by fitting the charge form factor of ^4He (calculated with the Morse potential) to older experimental data have also been reported in ref. [9].

In fitting the charge form factor the following cases were considered which led to the corresponding best fit values for the potential parameters (given in brackets):

Case I: The exact wave function was used in calculating the form factor and the RKB method for the center of mass correction ($a = 1.5501 fm^{-1}$, $d = 1.2262$ $(D = 74.9 MeV)$, $r_0 = 0.9216 fm$).

Case II: The approximate wave function was used and the RKB method for the centre of mass correction ($a = 1.6897 fm^{-1}$, $d = 1.1134$ $(D = 73.4 MeV)$, $r_0 = 0.9095 fm$).

Case III: The approximate wave function was used with the reduced mass, while in the previous cases the nucleon mass m was used instead of μ ($a = 1.5476 fm^{-1}$, $d = 1.4785$ $(D = 144.7 MeV)$, $r_0 = 0.8822 fm$).

In fitting the momentum distribution the following cases were considered (using the reduced mass):

Case a): The exact wave function was used in calculating the momentum distribution ($a = 2.2563 fm^{-1}$, $d = 1.0215$ $(D = 146.9 MeV)$, $r_0 = 0.3195 fm$).

Case b): The approximate wave function was used ($a = 2.1427 fm^{-1}$, $d = 0.8928$ $(D = 101.2 MeV)$, $r_0 = 0.5321 fm$).

It is seen from the above results that usually the best fit values of the parameters a and r_0 do not differ very much in each set of the above cases. There is, however, a more pronounced difference if the comparison is made between the corresponding best fit values of the first and the second set. It should be also noted that the value of ψ_0 (see section 2) is considerably smaller in case a) than in case I.

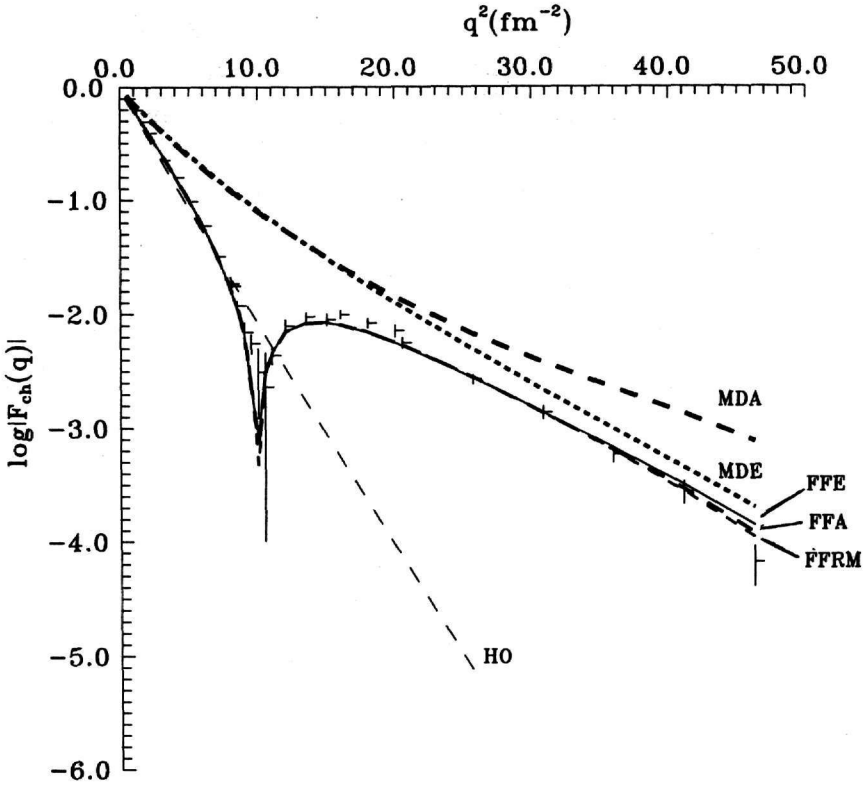

Fig 1.The charge form factor of ^{4}He for various cases (see text)

In figure 1, the variation of $log|F_{ch}(q)|$ with q^2 for ^4He is plotted for the cases I, II, and III, mentioned above. The corresponding curves are, FFE, FFA and FFRM, respectively. In the same figure the experimental data are shown by crosses. We notice that all three curves fit the experimental data well. In the same figure the results obtained calculating the form factor by using the best fit values of the potential parameters determined by fitting the momentum distribution are also shown. Thus, using the best fit values given in case a) above, the curve MDE is obtained. Using the best fit values given in case b), the curve MDA is obtained. We notice that the results are not good. This is a manifestation of the statement that one cannot fit simultaneously with a single-particle model, the form factor and the momentum distribution. Also, in the same figure we give the results obtained using the harmonic oscillator potential with potential parameter $b = 1.432fm$ determined by fitting the F_{ch} (curve HO). This is in fairly good agreement with the experimental data at

the small values of the momentum transfer, as is well known.

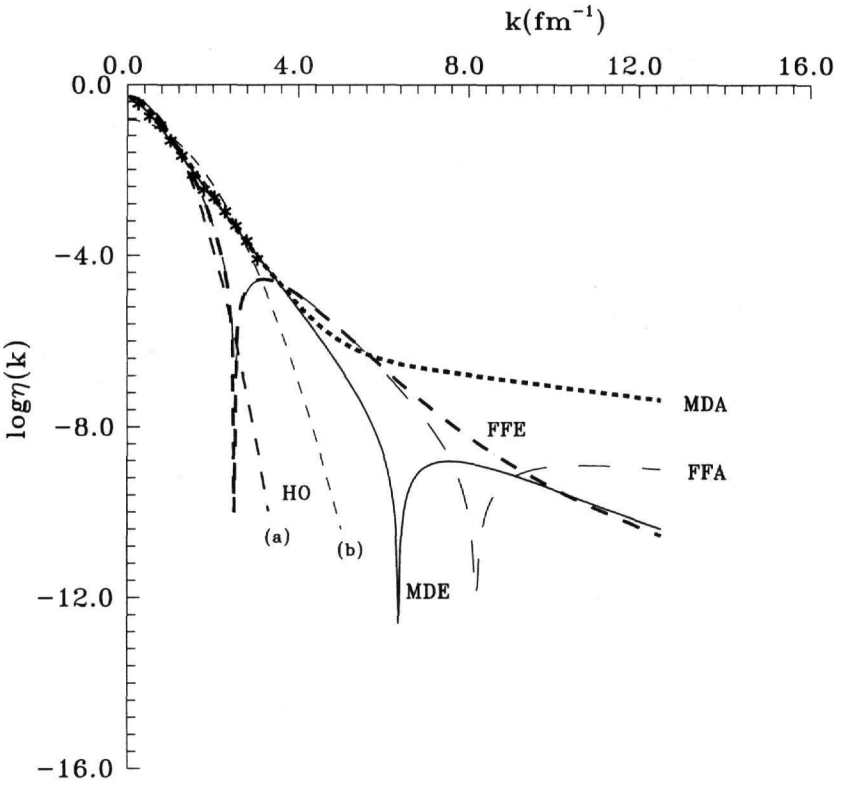

Fig 2.The nucleon momentum distribution of ^{4}He for various cases (see text)

In figure 2, the variation of the $log\eta(k)$ with k in ^4He is plotted for the cases a) and b), mentioned above. The corresponding curves are MDE and MDA, respectively. In the same figure the "experimental" points are shown by asteriscs. We see that both curves are in good agreement with the "experimental" data in the region where these results are known. The theoretical curves deviate from each other for the higher k values as one should expect. In the same figure, the results obtained calculating the momentum distribution, by using the best fit values of the potential parameters determined by fitting the charge form factor, are also shown. Thus, using the best fit values given in case I above the curve FFE is obtained, while using the best fit values given in case II above the curve FFA. Also, in the same figure we give the results obtained using the harmonic oscillator potential with $b = 1.432fm$ (curve HO(a)). It is seen that for the lower values of the momentum the agreement with the "ex-

perimental" data is not bad, but for the larger values there is the well known unrealistically steep decrease of $\eta(k)$. The situation is considerably improved if b is determined by fitting the $n(k)$ (see curve HO(b)) but the overall fit is still less satisfactory than that of MDE.

The body and charge density distributions of ^4He were also calculated using the exact and the approximate wavefunctions with the potential parameters indicated in cases I and II. The corresponding curves are shown in figure 3. In this figure $\rho_{Be}(r)$ is the body density distribution obtained using the exact wavefunction with potential parameters given in case I, while $\rho_{\mathrm{Ba}}(r)$ is the body density distribution using the approximate one with the potential parameters given in case II. $\rho_{ch}(r)(e)$ is the charge density distribution using the exact wave function with potential parameters given in case I and $\rho_{ch}(r)(a)$ is the charge density distribution using the approximate wavefunction with potential parameters given in case II.

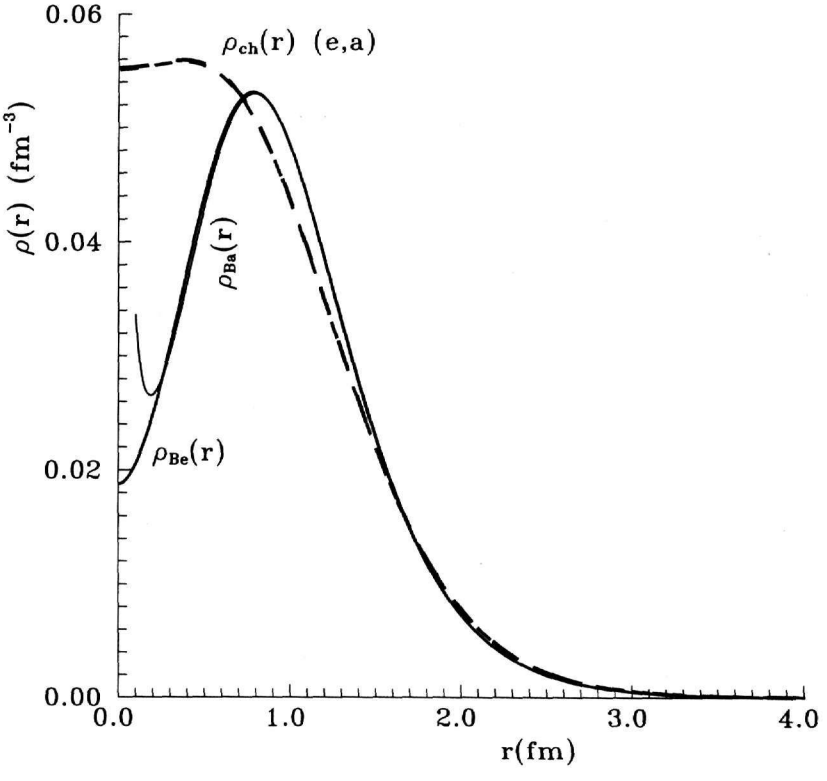

Fig 3.The charge ρ_{ch} point-proton (body) ρ_B density distributions of ^{4}He ob-

tained with the exact (e) and the approximate (a) wave functions.

It is seen that the analytic approximate expression for $\rho_{Ba}(r)$ is in good agreement with the exact one except for a small region near the origin $r \lesssim 0.2fm$. The pronounced dip of the point-proton density at small r is expected. It is due to the short range repulsion of the Morse potential. This is largely smeared out in the charge density because of the proton charge density.

The root mean square radii of these distributions are respectively :

$$< r^2 >^{1/2} (\rho_{Be}(r)) = 1.651fm$$

$$< r^2 >^{1/2} (\rho_{Ba}(r)) = 1.665fm$$

$$< r^2 >^{1/2} (\rho_{ch}(r)(e)) = 1.668fm$$

$$< r^2 >^{1/2} (\rho_{ch}(r)(a)) = 1.678fm$$

In conclusion, let us summarize the main results of the present investigation:

1) The Morse approximate analytic ground state single-particle wave function of the ^4He nucleus, when the parameters are determined by fitting the $F_{ch}(q)$, agrees fairly well with the corresponding (semi-analytic) exact one, except for a small region near the origin. This has the effect that certain quantities calculated with the approximate wavefunction such as $\rho_B(r)$ and $n(k)$ differ substantially, at small r and large k, respectively, from the corresponding values obtained by means of the exact wavefunction. However, this is not the case for the $\rho_{ch}(r)$ and the $log|F_{ch}(q)|$.

2) Although we can not fit simultaneously the form factor and the momentum distribution, because as is well known a single-particle wave function can not achieve this, considerable overall improvement is observed in comparison with the results obtained with the harmonic oscillator wave function.

3) The $< r^2 >^{1/2}$ of the charge density distribution is compared favourably with the values $1.671fm$ and $1.696fm$ obtained with model independent analysis [15].

Acknowledgment

This work was partly supported by the EEC under contract ERB-CIPA-CT-92-2231 and by the Greek General secretariat of Research and Technology (contract PENED No 360/91)

References

[1] A. N. Antonov, P. E. Hodgson and J. Zh. Petkov, Nucleon Momentum and Density Distributions in Nuclei, Clarendon Press, Oxford (1988).

[2] a) S. Frullani and J. Mougey, Adv. Nucl. Phys. Vol. **14** (1984) ed. by J. Negele and E. Vogt.

b) P. K. A. de Witt Huberts, J. Phys. G. Nucl. Part. Phys.**16** (1990) 507.

[3] a) O. Bohigas and S. Stringari, Physics Let. **95**B (1980) 9.

b) M. Dal Ri, S. Stringari and O. Bohigas , Nucl. Phys. A **376** (1982) 81.

c) M. Traini and G. Orlandini, Z. Phys. A**321** (1985) 479.

d) A. N. Antonov, Chr. V. Christov, I. Zh. Petkov, Nuovo Cim. **91**A (1986) 119.

e) R. Schiavilla, V. R. Pandharipande and R. B. Wiringa, Nucl. Phys. A**449** (1986) 219.

[4] C. Ciofi degli Atti, Nucl. Phys. A**497** (1989) 361C.

[5] a) M. E. Grypeos and K. N. Ypsilantis, J. Phys. G Nucl. and Part. Phys. **15** (1989) 1397

b) K. N. Ypsilantis, Ph. D. thesis, Aristotle University of Thessaloniki, Thessaloniki (1991).

c) K. N. Ypsilantis and M. E. Grypeos, J Phys. G Nucl. and Part. Phys. **21** (1995) 1701.

[6] P. Morse, Phys. Rev. **34** (1929) 57.

[7] D. Ter Haar, Phys. Rev.**70** (1946) 222.

[8] S. Flügge, Practical Quantum Mechanics I, p. 182, Springer-Verlag, Berlin, Heidelberg, New York 1971.

[9] A. Gersten and A. E. S. Green, Bull. Am. Phys. Soc. **13** (1968) 627.

[10] D. Bonatsos and C. Daskaloyannis, Phys. Let. **278** (1992) 1.

[11] F. Iachello and S. Oss, Phys. Rev. Let. **66** (1991) 2976.

[12] F. Iachello and S. Oss, Chem. Phys. Let. **187** (1991) 500.

[13] H. Chandra and G. Sauer, Phys. Rev. C **13** (1976) 245.

[14] S. Radhakant, S. Khadkikar and B. Banerjee, Nucl. Phys. A **142** (1970) 81.

[15] H. De Vries, C. W. de Jager and C. de Vries, Atomic Data and Nuclear Data Tables **36** (1987) 495.